

尿素对土壤水分传感器测量精度的影响

石玉娇¹ 尹 峥¹ 王红叶² 刘晓辰¹ 石庆兰^{1,3} 梅树立¹

(1. 中国农业大学信息与电气工程学院, 北京 100083; 2. 农业农村部耕地质量监测保护中心, 北京 100125;
3. 国家数字渔业创新中心, 北京 100083)

摘要: 土壤水分的精准测量对节水灌溉、墒情监测、水肥一体化等领域具有重要意义, 土壤氮含量会影响水分传感器的测量。为了消除这种影响, 设计了不同尿素质量对不同水分含量土壤样本的监测实验, 采用高灵敏度水分传感器并对尿素干扰下的输出电压进行监测, 通过称重法监测土壤样本的含水率, 使用 LCR 电桥测试仪监测土壤样本的电容和电阻。为了研究氮含量影响水分测量的机理, 根据实验数据建立了三元三次多项式、BP 神经网络、深度学习 3 种预测模型, 并对预测结果进行误差分析。结果表明, 相同土壤含水率条件下, 尿素质量与土壤水分传感器输出值呈周期性的振荡关系。3 种预测模型的平均绝对误差分别为 0.77%、0.64%、0.75%, BP 神经网络模型有 98% 误差集中在 0~2% 区间, 误差峰值仅为 2.07%, 确立 BP 神经网络模型为最佳抗尿素干扰水分预测模型。

关键词: 土壤水分传感器; 尿素; 多项式回归; BP 神经网络; 深度学习

中图分类号: S151.9; S126 **文献标识码:** A **文章编号:** 1000-1298(2020)S2-0388-07

Effect of Urea on Measurement Accuracy of Soil Moisture Sensor

SHI Yujiao¹ YIN Zheng¹ WANG Hongye² LIU Xiaochen¹ SHI Qinglan^{1,3} MEI Shuli¹

(1. College of Information and Electrical Engineering, China Agricultural University, Beijing 100083, China
2. Center of Cultivated Land Quality Monitoring and Protection, Ministry of Agriculture and Rural Affairs, Beijing 100125, China
3. National Innovation Center for Digital Fishery, Beijing 100083, China)

Abstract: The accurate measurement of soil moisture is of great significance to the fields of water-saving irrigation, moisture monitoring, water and fertilizer integration, and the soil nitrogen content will affect the measurement of the moisture sensor. In order to eliminate this effect, a monitoring experiment of different urea on soil samples with different moisture contents was designed, a high-sensitivity moisture sensor was used to monitor the output voltage value under the interference of urea, and the moisture content of the soil sample was monitored by weighing method, the capacitance and resistance of the soil sample was monitored by LCR bridge tester. Totally 800 sets of sample data were obtained, of which 75% were used as the training set and 25% were used as the validation set. In order to study the mechanism of the influence of nitrogen content on moisture measurement, three predictive models, including a three-element cubic polynomial model, a BP neural network model, and a deep learning model, were established based on experimental data, and error analysis was performed on the prediction results. The analysis showed that the highest errors of the three models were 2.86%, 2.07% and 3.82%, and the errors were concentrated in the range of 0 to 2%, accounting for 89%, 98% and 90%, respectively. The following conclusions were obtained: different urea contents had different influences on the predicted value, which was roughly in a periodic oscillation relationship. When the soil moisture content was lower, the interference of urea content on voltage was greater, and the same was true for impedance, but capacitive reactance was only sensitive to soil moisture, but not to changes in urea. Therefore, the interference of urea on soil moisture measurement was mainly caused by interference with soil resistance. The average absolute errors of the three-dimensional cubic polynomial, BP neural network, and deep learning models were 0.77%, 0.64% and 0.75%, respectively, and BP neural

收稿日期: 2020-08-06 修回日期: 2020-09-13

基金项目: 国家自然科学基金项目(61871380)

作者简介: 石玉娇(1992—), 女, 硕士生, 主要从事土壤氮含量检测研究, E-mail: 370772906@qq.com

通信作者: 石庆兰(1965—), 女, 副教授, 主要从事土壤墒情监测研究, E-mail: shiql@cau.edu.cn

network model was the most stable, with the most prediction results concentrated in the low error range. No matter how the urea content changed, the BP neural network prediction value curve can always track the actual mass moisture content curve very well. BP neural network model was superior to other network models in terms of prediction accuracy and stability. Therefore, BP neural network moisture prediction model was established as the best anti-urea interference model. The interference of nitrogen content on moisture measurement was eliminated by increasing the data dimension and the prediction model was established, and the prediction accuracy was improved.

Key words: soil moisture sensor; urea; polynomial regression; BP neural network; deep learning

0 引言

土壤水分的实时、精准、稳定监测对节水灌溉、水肥一体化以及土壤墒情监测等领域都具有重要意义,是农业物联网、大数据的技术关键。土壤水分传感器也是水肥一体化自动灌溉过程中重要的监测设备,用于监测水肥灌溉量及其运移情况。在农业实际生产过程中田间环境和气象因素多变、土壤空间变异性较大、土壤施肥等复杂因素会导致传感器的测量受到干扰。

目前,关于影响土壤水分传感器测量精度的研究较多地集中在温度、土壤质地以及土壤盐分。而对土壤中各种养分对土壤水分传感器影响的研究极为少见。

诸多学者在温度对基于各种不同检测原理的土壤水分传感器的影响方面基本都有所研究,并给出解决方案^[1-3]。此外,一些学者对影响传感器测量精度的环境电磁特性、土壤温度、土壤盐分与土壤容重等因素进行了研究,并建立了相关模型^[4-10]。文献[11-12]发现土壤中尿素含量的变化会引起土壤介电常数的变化并设计了一款基于频域(Frequency domain, FD)原理的土壤尿素测量传感器。虽然土壤氮含量检测的研究众多^[13-19],但至今仍未见有关介电法传感器对氮含量实时在线监测的研究报道。氮是土壤养分中占比较大的元素,直接影响植物的生长、产量和品质。而尿素是含氮量较高、易溶于水、农业生产中普遍使用的有机态氮肥,水肥一体化灌溉中的水肥相互耦合相互影响,会导致土壤水分传感器测量精度受到影响。本文建立预测模型以校准土壤水分含量测量值。

1 不同尿素含量下土壤水分与传感器介电参数变化关系的监测实验

为了确定土壤中尿素含量对土壤水分传感器的影响,连续监测在不同尿素含量下土壤水分从接近饱和到自然风干过程中与传感器介电参数间的关系,实验采用自主研发的高灵敏度土壤水分传感器^[20-21],其特点是对土壤介电常数的变化很敏感,

能够捕捉 0.1% 的水分变化。实验步骤如下:

(1) 制备实验样本,实验所用土壤取自中国农业大学(东校区)附近(北纬 40°,东经 116°)地表下 20~40 cm 土壤,土壤粒径组成为粗粒质量分数 68.6%,粉粒质量分数 25% 和粘粒质量分数 6.4% 的砂质壤土,风干过 1 mm 孔径筛后置于 105℃ 恒温的 101-2 型电热恒温鼓风干燥箱中干燥 12 h,待土壤温度降至室温作为实验待测样本。

(2) 称取干燥后的 7 kg 土壤倒入直径为 50 cm、高 20 cm 的铁盆中平整摊匀,再用定量尿素(尿素含氮质量分数 46%)与自来水混合配成的一定浓度的溶液与干燥土混合,搅拌均匀制成饱和含水率的待测土壤样本。

(3) 使用长为 15 cm 筒状化纤口袋套在直径为 15 cm、深度为 20 cm 的聚氯乙烯(Polyvinyl chloride, PVC)桶内(简称实验桶,用于前期土壤水分含量较高时固定土柱形状)。将传感器立于实验桶中间,将全部待测土壤分层装入桶中,并在每层土壤装入时都用实心柱棒砸实,目的是为了将土壤中的空气挤出。

(4) 当全部待测土壤装入桶中砸实后即完成传感器的安装,将安装了传感器的实验桶称量,记录总质量并计算初始土壤含水率。

(5) 传感器开机,传感器的电压输出自动上传云平台,采样周期为 1 h,采用称重法监测含水率变化,每隔 2 h 一次。采用常州市优策电子科技有限公司生产的电感电容电阻(Lenz capacitor resistance, LCR)电桥测试仪(UC2836A 型)进行土柱电阻 R 、电容 C 的检测。仪器频率设置为 15 kHz,电平设置为 300.0 mV,内阻设置为 30 Ω ,可以同时检测电阻与电容,基本测试精度为 0.05%。使用四端开尔文测试电缆将待测物接入仪器进行检测。

(6) 实验初期由于土壤水分饱和土柱不成形无法站立,待大约 7 d 后,土壤质量含水率约下降至 20% 时,土柱形状基本固定。为使土壤水分风干速度更快,将土柱连同化纤口袋从 PVC 桶中取出。为防止土柱变形或因土壤过干而龟裂,用绳子将口袋扎紧。经过约 25 d 自然风干至土壤质量含水率接

近1%,实验结束。

(7)改变尿素含量,重新配制土壤样本,重复以上实验步骤。

实验测量过程示例如图1所示。

图2是6组尿素质量分别为0、1、3、5、7、10g下土壤含水率从饱和到自然风干过程的传感器电压输出变化值,随着土壤中加入尿素质量的变化,不仅影响了土壤水分传感器的输出值,同时影响了电阻、电容监测仪的输出值,监测参数的变化是波动的。

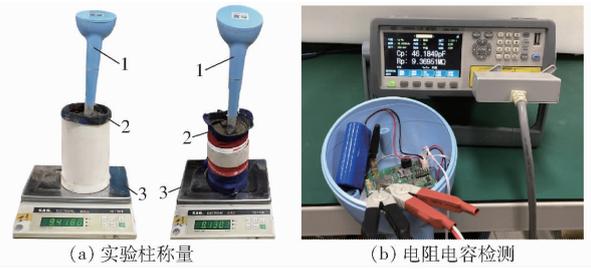


图1 实验过程示例

Fig. 1 Example of experimental procedure

1. 传感器 2. 无纺布袋 3. PVC 桶

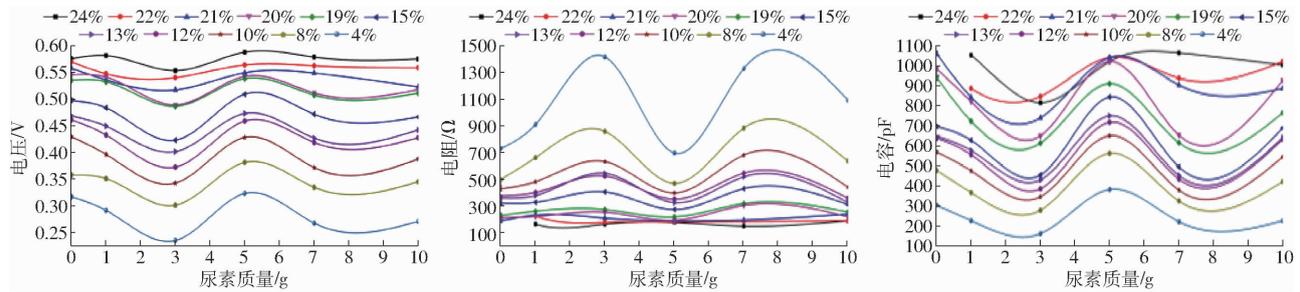


图2 不同含水率条件下尿素质量与传感器参数的关系

Fig. 2 Relationships between urea quality and sensor parameters under different moisture content

对上述实验所获取的6种不同尿素质量土壤水分及传感器介电参数的数据进行无量纲化预处理。

无量纲化相关数据如表1、2所示。总计有800条数据,其中75%数据作为训练集,25%作为验证集。

表1 实验数据的数学期望值及方差

Tab. 1 Mathematical expected value and variance of experimental data

土壤含水率		电压 U		电阻 R		电容 C	
数学期望 μ_{WCS}	标准差 δ_{WCS}	数学期望 μ_U	标准差 δ_U	数学期望 μ_R	标准差 δ_R	数学期望 μ_C	标准差 δ_C
10.8466	8.1539	0.3740	0.1328	928.2345	987.0637	513.0128	321.4026

表2 土壤含水率及传感器介电参数的数据无量纲化预处理示例

Tab. 2 A sample pretreatment of soil moisture and dielectric parameters of sensor by normalization

日期	时刻	原始记录值				标准化值			
		土壤含水率/ %	电压 U/V	电阻 R/Ω	电容 C/pF	土壤含水率	电压 U	电阻 R	电容 C
2018年 11月5日	17:08	25.5656	0.556	174.0	1200	1.805151	1.3709	-0.7641	2.1375
	19:15	23.7145	0.551	179.0	1070	1.578131	1.3332	-0.7590	1.7330
	21:21	24.9225	0.547	182.4	1060	1.726281	1.3031	-0.7556	1.7019
	22:24	24.8425	0.545	184.0	1060	1.716470	1.2880	-0.7540	1.7019

2 预测模型建立

从监测数据可以得到在不添加尿素时传感器电压与土壤含水率三次项拟合的关系方程为

$$WCS_{pre}(U_1) = 39.755U_1^3 - 26.84U_1^2 + 21.449U_1 - 5.032 \quad (R^2 = 0.9979) \quad (1)$$

式中 WCS_{pre} ——土壤含水率预测值

U_1 ——传感器电压

但是在添加了尿素以后的监测值都偏离了0g曲线,表明测量误差加大。下面将针对添加尿素而引起的误差进行校准以提高测量精度,对以上监测

值建立抗干扰校准模型。

2.1 三元三次多项式回归预测模型

以监测数据电压、电阻、电容作为三元三次多项式模型的输入参数,得到方程为

$$WCS_{pre}(X) = \sum_{i=0}^n w_i x_i = W^T X \quad (2)$$

式中 X ——由 $U、R、C$ 通过不同的排列组合得到的次数为3的向量

x_i ——输入参数 w_i ——模型参数

W —— w_i 的矩阵形式

本文中排列组合种类 $n = 19$,所以多项式回归

中特征值的维度为 20 维。将多元多次多项式回归问题转换为线性回归问题,其参数求解方法,采用线性回归求解方式进行求解。其求解方式与原理即线性回归求解方式与原理。由于进行的是三元三次多项式回归,回归所用特征向量的维度高达 20 维,为预防过拟合问题,算法加入了 L2 正则化惩罚项。其权重更新过程如下:

线性回归损失函数为

$$J(\mathbf{W}) = \frac{1}{2m} \sum_{i=1}^m (\text{WCS}_{\text{pre}}(\mathbf{X})^{(i)} - \text{WCS}_{\text{mv}}(\mathbf{X})^{(i)})^2 + \frac{1}{2m} \lambda \sum_{i=1}^m \|w_j\|^2$$

式中 m ——样本个数

$\text{WCS}_{\text{pre}}(\mathbf{X})^{(i)}$ ——第 i 个样本的土壤含水率预测值 $\text{WCS}_{\text{pre}}(\mathbf{X})$

$\text{WCS}_{\text{mv}}(\mathbf{X})^{(i)}$ ——第 i 个样本的土壤含水率期望值 $\text{WCS}_{\text{mv}}(\mathbf{X})$

w_j ——第 j 个特征的权值参数, $j=0,1,\dots,19$

λ ——惩罚力度, λ 越大,惩罚力度越大,拟合曲线(曲面)越平缓

其求解原理为

$$\frac{dJ(\mathbf{W})}{d\mathbf{W}} = \mathbf{X}^T \mathbf{X} \mathbf{W} - \mathbf{X}^T \text{WCS}_{\text{mv}}(\mathbf{X}) + \lambda \mathbf{W}$$

令 $\frac{dJ(\mathbf{W})}{d\mathbf{W}} = 0$, 解得

$$\mathbf{W} = (\mathbf{X}^T \mathbf{X} + \lambda)^{-1} \mathbf{X}^T \text{WCS}_{\text{mv}}(\mathbf{X})$$

2.2 BP 神经网络预测模型

采用反向传播(Back propagation, BP)神经网络预测土壤水分含量,其结构如图 3 所示。归一化后的 U, R, C 作为输入层。图中, b_1 为输入层的偏置量,初始值为 0, \mathbf{W}_1 为输入层到隐藏层间的 $3 \times n$ 的权值参数矩阵, \mathbf{Z}_1 为 $m \times n$ 矩阵, f 为激活函数,为实现神经网络的非线性特点,选用线性整流(Rectified linear unit, ReLu)函数作为激活函数, \mathbf{W}_2 为隐藏层

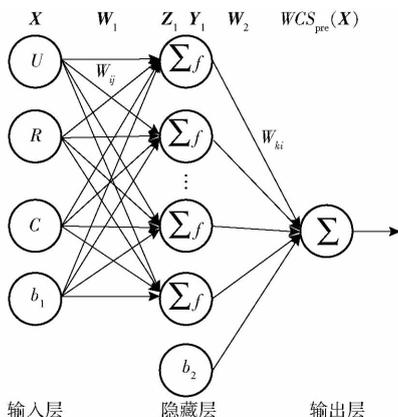


图 3 BP 神经网络结构

Fig. 3 BP neural network structure

到输出层间的 $n \times 1$ 的权值参数矩阵。

(1) 前向传播

输入层为

$$\mathbf{X} = [\mathbf{U} \quad \mathbf{R} \quad \mathbf{C}]$$

隐藏层为

$$\mathbf{Z}_1 = \mathbf{W}_1 \mathbf{X} + b_1$$

$$\mathbf{Y}_1 = \max(0, \mathbf{Z}_1)$$

输出层为

$$\text{WCS}_{\text{pre}}(\mathbf{X}) = \mathbf{W}_2 \mathbf{Y}_1 + b_2$$

(2) 反向传播

当神经网络用于回归预测任务时,一般选用均方差作为损失函数。通过样本数据的训练,不断修正模型求解参数,使得 $\text{WCS}_{\text{pre}}(\mathbf{X})$ 逼近期望输出值 $\text{WCS}_{\text{mv}}(\mathbf{X})$ 。本文仅以此公式推导过程阐述算法实现流程,为使公式易于理解,假设每批次输入样本数量为 1 进行公式推导。

均方差损失函数为

$$C_X = \frac{1}{2} (\text{WCS}_{\text{pre}}(\mathbf{X}) - \text{WCS}_{\text{mv}}(\mathbf{X}))^2$$

对于输出层

$$\delta_2 = \frac{\partial C_X}{\partial \text{WCS}_{\text{pre}}(\mathbf{X})} = \text{WCS}_{\text{pre}}(\mathbf{X}) - \text{WCS}_{\text{mv}}(\mathbf{X})$$

$$\frac{\partial C_X}{\partial b_2} = \frac{\partial C_X}{\partial \text{WCS}_{\text{pre}}(\mathbf{X})} \frac{\partial \text{WCS}_{\text{pre}}(\mathbf{X})}{\partial b_2} =$$

$$\text{WCS}_{\text{pre}}(\mathbf{X}) - \text{WCS}_{\text{mv}}(\mathbf{X}) = \delta_2$$

$$\frac{\partial C_X}{\partial \mathbf{W}_2} = \frac{\partial C_X}{\partial \text{WCS}_{\text{pre}}(\mathbf{X})} \frac{\partial \text{WCS}_{\text{pre}}(\mathbf{X})}{\partial \mathbf{W}_2} =$$

$$(\text{WCS}_{\text{pre}}(\mathbf{X}) - \text{WCS}_{\text{mv}}(\mathbf{X})) \mathbf{Y}_1 = \delta_2 \mathbf{Y}_1$$

对于隐藏层

$$\delta_1 = \frac{\partial C_X}{\partial \mathbf{Z}_1} = \frac{\partial C_X}{\partial \text{WCS}_{\text{pre}}(\mathbf{X})} \frac{\partial \text{WCS}_{\text{pre}}(\mathbf{X})}{\partial \mathbf{Y}_1} \frac{\partial \mathbf{Y}_1}{\partial \mathbf{Z}_1} =$$

$$(\text{WCS}_{\text{pre}}(\mathbf{X}) - \text{WCS}_{\text{mv}}(\mathbf{X})) \mathbf{W}_2 \odot \mathbf{Y}'_1$$

其中

$$\mathbf{Z}_1 = \mathbf{W}_1 \mathbf{X} + b_1$$

$$\mathbf{Y}'_1 = \begin{cases} 1 & (\mathbf{Z}_1 \geq 0) \\ 0 & (\mathbf{Z}_1 < 0) \end{cases}$$

其中 \odot 表示向量或矩阵对应位置的数相乘。

$$\frac{\partial C_X}{\partial b_1} = \frac{\partial C_X}{\partial \mathbf{Z}_1} \frac{\partial \mathbf{Z}_1}{\partial b_1} = (\text{WCS}_{\text{pre}}(\mathbf{X}) - \text{WCS}_{\text{mv}}(\mathbf{X})) \mathbf{W}_2 \odot \mathbf{Y}'_1 = \delta_1$$

$$\frac{\partial C_X}{\partial \mathbf{W}_1} = \frac{\partial C_X}{\partial \mathbf{Z}_1} \frac{\partial \mathbf{Z}_1}{\partial \mathbf{W}_1} = (\text{WCS}_{\text{pre}}(\mathbf{X}) -$$

$$\text{WCS}_{\text{mv}}(\mathbf{X})) \mathbf{W}_2 \odot \mathbf{Y}'_1 \mathbf{X} = \delta_1 \mathbf{X}$$

权值更新

$$\mathbf{W}_1 = \mathbf{W}_1 - \alpha \delta_1 \mathbf{X}$$

$$b_1 = b_1 - \alpha \delta_1$$

$$\mathbf{W}_2 = \mathbf{W}_2 - \alpha \delta_2 \mathbf{Y}_1$$

$$b_2 = b_2 - \alpha \delta_2$$

式中 α ——学习率,取 10^{-3}

采用均方根误差 (Root mean square error, RMSE)作为最终模型的评估指标。

2.3 深度学习预测模型

为了得到更高的预测精度,在 BP 神经网络单

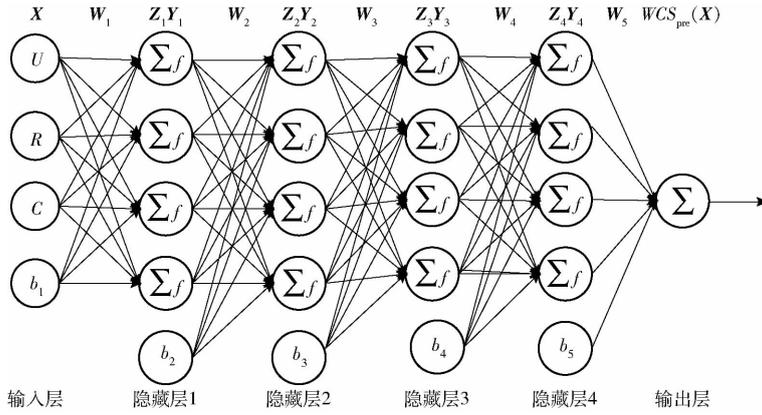


图4 深度学习神经网络结构

Fig.4 Deep learning neural network structure

2.4 误差分析

分别对 6 种不同尿素质量在不同含水率条件下的土壤样本测试集数据进行了预测,4 种预测模型得到的预测值与实际称重法得到的真实含水率关系如图 5 所示。可以看出,采用传统的一元三次多项式的标定方法,当土壤中加入尿素时含水率预测值偏离中心标准线,且尿素质量不同偏离程度也不同,如图 5a 所示。在增加了数据维度(土柱的电阻 R 和电容 C)之后分别得到的三元三次多项式、BP 神经网络和深度学习的预测值如图 5b ~ 5d 所示,与图 5a 相比有明显的收

敛。其中,采用 BP 神经网络的预测值与标准线的距离收敛最好。4 种模型得到的绝对误差概率分布情况如图 6 所示,绝对误差与期望值对比如图 7 所示。传统的一元三次多项式的标定方法在尿素干扰的情况下预测误差峰值高达 4.55%,且仅有 77% 误差范围集中在 0 ~ 2% 之间。在增加了二维监测参数后的三元三次多项式预测误差最高约 2.86%,且 89% 误差范围集中在 0 ~ 2% 之间。其最高绝对误差比一元三次多项式降低了 1.69 个百分点,且在误差概率分布上也集中于更小的误差范围。因此,增加数据测量

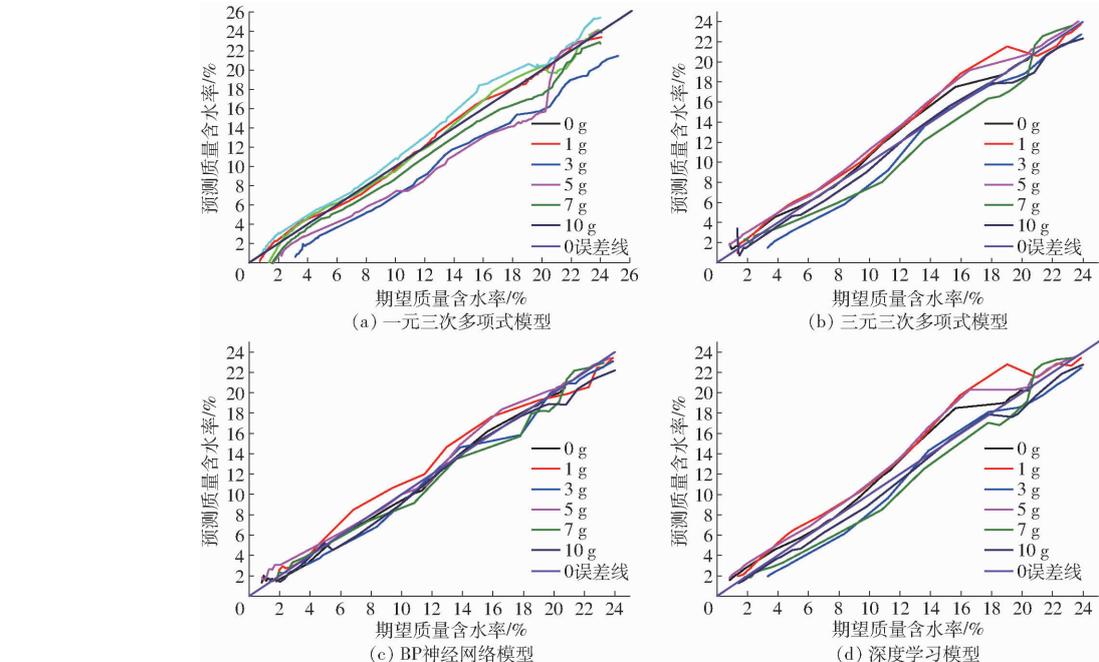


图5 土壤含水率预测值与期望值对比结果

Fig.5 Comparisons of predicted and expected values of soil moisture content

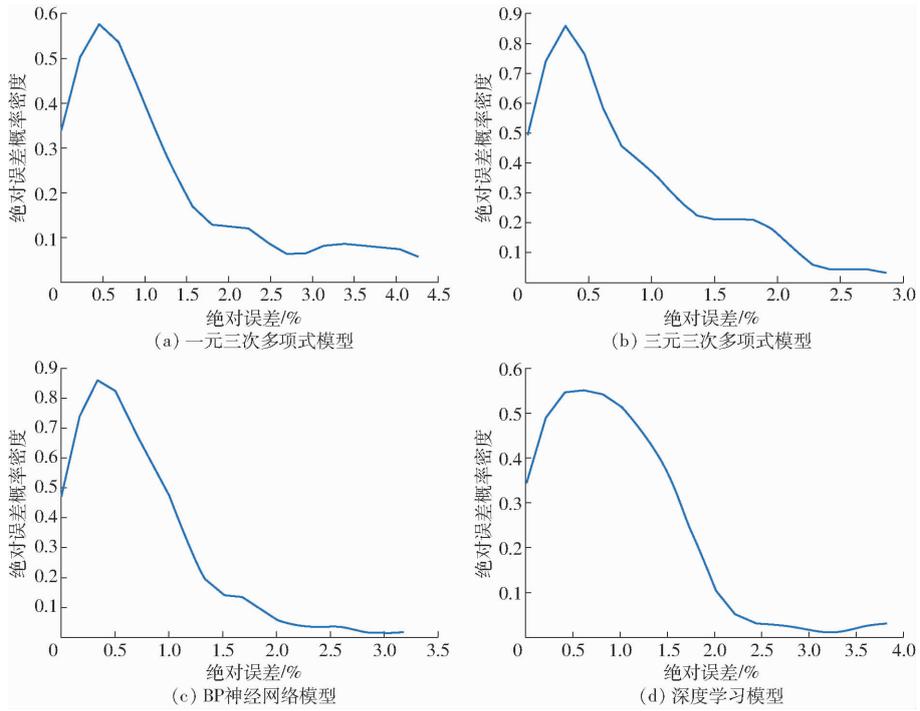


图 6 土壤含水率预测值与期望值绝对误差概率分布

Fig. 6 Probability distributions of absolute error between predicted and expected values of soil moisture content

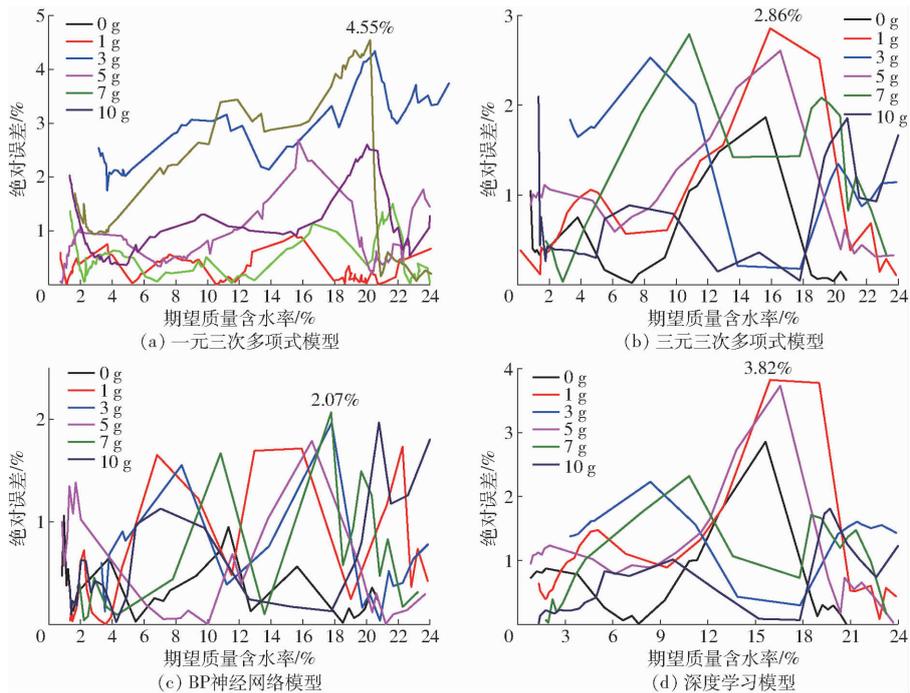


图 7 土壤含水率绝对误差与期望值对比

Fig. 7 Comparisons of absolute error of soil moisture content and expected value

维度,可有效提高土壤水分传感器的抗土壤尿素干扰性能。

三元三次多项式、BP 神经网络、深度学习 3 种模型的平均绝对误差分别为 0.77%、0.64%、0.75%。BP 神经网络预测模型的预测误差最高仅 2.07%,平均绝对误差基本稳定在 0.5% 左右,且 98% 误差范围集中在 0~2%。在误差概率分布上较三元三次多项式模型集中于更小的误差范围。

深度学习预测模型绝对误差概率分布中其最大绝对误差为 3.82%,且 90% 误差范围集中在 0~2%,深度学习神经网络模型的预测结果比一元三次多项式模型稳定,但是其并未因为模型复杂度和训练参数的增多而使得预测结果比简单的 BP 神经网络模型和三元三次多项式模型预测结果更稳定、更精确,需要进一步实验获取更多样本数据来验证。

3 结论

(1)在土壤中加入尿素时会使传感器的水分预测值偏离真实值,不同的尿素质量对预测值的影响程度不同,大致呈周期性的振荡关系。土壤含水率越低时尿素质量对土壤水分传感器输出电压的干扰越大,对土壤的电阻干扰也是如此,但土壤的电容是水分检测电路的敏感器件,尿素对其干扰随含水率变化却不大,说明传感器的敏感器件(感知环的容抗)仅对土壤水分敏感,而对尿素的变化量不敏感。因此尿素对土壤水分测量的干扰主要是通过干扰土

体电阻而发生作用。

(2)三元三次多项式、BP神经网络、深度学习3种模型的平均绝对误差分别为0.77%、0.64%、0.75%,且BP神经网络模型最稳定,有98%误差范围集中在0~2%。尿素质量变化时BP神经网络预测值曲线始终可以很好地跟踪实际质量含水率曲线,因此在预测精度和稳定性上,BP神经网络模型优于其他网络模型。确立BP神经网络含水率预测模型为最佳抗尿素干扰模型。

(3)通过增加数据维度后建立的预测模型消除了尿素对水分测量的干扰,提高了预测精度。

参 考 文 献

- [1] 张荣标,刘骏,张磊,等. EC-5土壤水分传感器温度影响机理及补偿方法研究[J]. 农业机械学报, 2010, 41(9): 168-172.
ZHANG Rongbiao, LIU Jun, ZHANG Lei, et al. Study on the influence mechanism and compensation method of EC-5 soil moisture sensor temperature[J]. Transactions of the Chinese Society for Agricultural Machinery, 2010, 41(9): 168-172. (in Chinese)
- [2] OATES M J, FERNÁNDEZ-LPEZ A, FERRÁNDEZ-VLLENA M, et al. Temperature compensation in a low cost frequency domain (capacitance based) soil moisture sensor[J]. Agricultural Water Management, 2016, 183(9): 86-93.
- [3] PALAPARTHY V S, SINGH D N, BAGHINI M S. Compensation of temperature effects for in-situ soil moisture measurement by DPHP sensors[J]. Computers and Electronics in Agriculture, 2017, 141: 73-80.
- [4] 郭文川,宋克鑫,张鹏,等. 土壤温度和容重对频率反射土壤水分传感器测量精度的影响[J]. 农业工程学报, 2013, 29(10): 136-143.
GUO Wenchuan, SONG Kexin, ZHANG Peng, et al. Effects of temperature and bulk density on measurement precision of soil moisture sensor based on frequency domain reflectometry[J]. Transactions of the CSAE, 2013, 29(10): 136-143. (in Chinese)
- [5] 陈海波,冶林茂. 土质对FDR水分传感器拟合参数影响的试验研究[J]. 气象科技, 2014, 42(5): 888-892.
CHEN Haibo, YE Linmao. Experimental research on effect of soil texture on fitting parameters of FDR moisture sensors[J]. Meteorological Science and Technology, 2014, 42(5): 888-892. (in Chinese)
- [6] SAITO T, FUJIMAKI H, INOUE M. Calibration and simultaneous monitoring of soil water content and salinity with capacitance and four-electrode probes[J]. American Journal of Environmental Sciences, 2008, 4(6): 683-692.
- [7] 叶智杰,洪添胜,JOSEPH M C,等. EC-5和5TE土壤水分传感器的多因素性能测试与校正[J]. 农业工程学报, 2012, 28(10): 157-166.
YE Zhijie, HONG Tiansheng, JOSEPH M C, et al. Multi-factor evaluation and modeling correction of EC-5 and 5TE soil moisture content sensors[J]. Transactions of the CSAE, 2012, 28(10): 157-166. (in Chinese)
- [8] 刘蓓. 土壤含盐量和温度对FDR土壤水分传感器检测模型的影响研究[D]. 杨凌: 西北农林科技大学, 2014.
LIU Bei. Study on the influence of soil salinity and temperature on FDR soil moisture sensor detection model[D]. Yangling: Northwest A&F University, 2014. (in Chinese)
- [9] BERNARD C, DUKES M D. Effect of temperature and salinity on the precision and accuracy of landscape irrigation soil moisture sensor systems[J]. Journal of Irrigation and Drainage Engineering, 2015, 141(7): 4014076.
- [10] 贺蕾. 微型TDR土壤水分传感器影响因素研究及其应用模型建立[D]. 乌鲁木齐: 新疆农业大学, 2016.
HE Lei. Study on influencing factors of micro TDR soil moisture sensor and establishment of its application model[D]. Urumqi: Xinjiang Agricultural University, 2016. (in Chinese)
- [11] 刘卫平. 土壤中尿素含量与介电常数关系的研究[D]. 北京: 北京林业大学, 2013.
LIU Weiping. Study on the relationship between urea content and dielectric constant in soil[D]. Beijing: Beijing Forestry University, 2013. (in Chinese)
- [12] 董晓晨,刘卫平,皮婷婷,等. 基于FDR原理的土壤氮含量检测方法研究[J]. 中国农学通报, 2014, 30(36): 204-210.
DONG Xiaochen, LIU Weiping, PI Tingting, et al. Detection method of soil nitrogen content based on FDR theory[J]. Chinese Agricultural Science Bulletin, 2014, 30(36): 204-210. (in Chinese)
- [13] KJELDAHL J. Neue methode zur bestimmung des stickstoffs in organischen körpern[J]. Zeitschrift für Analytische Chemie, 1883, 22(1): 366-382.

- sensing component[C]//European Conference on Precision Agriculture, 2005.
- [14] ADAMCHUK V I, LUND E D, SETHURAMASAMYRAJA B, et al. Direct measurement of soil chemical properties on-the-go using ion-selective electrodes[J]. *Computers & Electronics in Agriculture*, 2005, 48(3): 272–294.
- [15] ADAMCHUK V I, LUND E D, REED T M, et al. Evaluation of an on-the-go technology for soil pH mapping[J]. *Precision Agriculture*, 2007, 8(3): 139–149.
- [16] SETHURAMASAMYRAJA B, ADAMCHUK V I, MARX D B, et al. Analysis of an ion-selective electrode based methodology for integrated on-the-go mapping of soil pH, potassium, and nitrate contents[J]. *Transactions of ASABE*, 2007, 50(6): 1927–1935.
- [17] SETHURAMASAMYRAJA B, ADAMCHUK V I, DOBERMANN A, et al. Agitated soil measurement method for integrated on-the-go mapping of soil pH, potassium and nitrate contents[J]. *Computers & Electronics in Agriculture*, 2008, 60(2): 212–225.
- [18] ALVES A P P, KOIZUMI R, SAMANTA A, et al. One-step electrodeposited 3d-ternary composite of zirconia nanoparticles, RGO and polypyrrole with enhanced supercapacitor performance[J]. *Nano Energy*, 2016, 31: 225–232.
- [19] UMAR M F, NASAR A. Reduced graphene oxide/polypyrrole/nitrate reductase deposited glassy carbon electrode (GCE/RGO/PPy/NR): biosensor for the detection of nitrate in wastewater[J]. *Applied Water Science*, 2018, 8(7): 211.
- [20] WANG J, MAO S, LI H F, et al. Multi-DNAzymes functionalized on gold nanoparticles by rolling circle amplification for highly sensitive detection of thrombin on microchip[J]. *Anal. Chim. Acta*, 2018, 1027: 76–82.
- [21] CHEN M, ZHANG M, WANG X M, et al. An all-solid-state nitrate ion-selective electrode with nanohybrids composite films for in-situ soil nutrient monitoring[J]. *Sensors*, 2020, 20(8): 2270.
- [22] UMEZAWA Y, BUHLMANN P, UMEZAWA K, et al. Potentiometric selectivity coefficients of ion-selective electrodes Part II. Inorganic cations (technical report)[J]. *Pure & Applied Chemistry*, 2002, 74(6): 923–994.
- [23] LI Y, YANG Q, CHEN M, et al. An ISE-based on-site soil nitrate nitrogen detection system[J]. *Sensors*, 2019, 19(21): 4669.
-

(上接第 394 页)

- [14] SHAN H, HAILUN Z, REZA S A, et al. Spatiotemporal variability of soil nitrogen in relation to environmental factors in a low hilly region of southeastern China[J]. *International Journal of Environmental Research and Public Health*, 2018, 15(10): 2113.
- [15] KIM H J, HUMMEL J W, BIRRELL S J. Evaluation of ion-selective membranes for real-time soil nutrient sensing[C]//Agricultural and Biosystems Engineering Conference Proceedings and Presentations, 2003.
- [16] VOHLAND M, LUDWIG M, THIELE-BRUHN S, et al. Determination of soil properties with visible to near- and mid-infrared spectroscopy: effects of spectral variable selection[J]. *Geoderma*, 2014, 223(1): 88–96.
- [17] KULKARNI M Y, WARHADE K K, BAHEKAR S K. Primary nutrients determination in the soil using UV spectroscopy[J]. *International Journal of Emerging Engineering Research and Technology*, 2014, 2(2): 198–204.
- [18] 张瑶, 李民赞, 郑立华, 等. 基于近红外光谱分析的土壤分层氮素含量预测[J]. *农业工程学报*, 2015, 31(9): 121–126.
ZHANG Yao, LI Minzan, ZHENG Lihua, et al. Prediction of soil total nitrogen content in different layers based on near infrared spectral analysis[J]. *Transactions of the CSAE*, 2015, 31(9): 121–126. (in Chinese)
- [19] PUNO J C V, BANDALA A A, DADIOS E P, et al. Vision system for soil nutrient detection using fuzzy logic[C]//TENCON 2018—2018 IEEE Region 10 Conference. IEEE, 2018.
- [20] SAEED I A, SHI Qinglan, WANG Minjuan, et al. Development of a low-cost multi-depth real-time soil moisture sensor using time division multiplexing approach[J]. *IEEE Access*, 2019, 7: 19688–19697.
- [21] AHMAD I. Integrated sensor for estimating in situ soil water content in vertical profile[J]. *Journal of Agricultural Science*, 2018, 10(10): 53.